

Automated Processing of Colour Stereo Georeferenced Images for Road Inventory

Krzysztof GAJDAMOWICZ
 Dept. of Geodesy and Photogrammetry
 Royal Institute of Technology,
 Drottning Kristinas Väg 32, S-100 44 Stockholm
 E-mail: krzygajd@geomatics.kth.se
 SWEDEN

Commission V, Working Group IC WG/III

KEY WORDS: GIS Data Acquisition, Road Inventory, Colour Image Analysis, Colour Based Segmentation, Property Based Matching, Automatic Shape Detection.

ABSTRACT

Road inventory with a Mobile Mapping System (MMS) consists of two basic steps: data acquisition and data post-processing. The data, colour stereo georeferenced images, is captured by Colour Progressive Scan CCD cameras which are integrated and time tagged with GPS/INS. Collected information is analysed in a post-process in order to obtain information about roads and road signs. This paper presents an overview of the road inventory system (MMS) and describes in detail the data processing module for road inventory and automatic inventory of road signs from colour stereo georeferenced images.

The inventory from georeferenced stereo images is performed in two basic alternatives: semiautomatic and automatic. The semiautomatic alternative is designed for task survey (a single point 3D measurements). This approach demands interaction between operator and software. In order to perform 3D measurement, a point has to be selected in one of the stereo images. The epipolar line is then calculated in the second image. The corresponding point is found along the line with template matching or by manual selection performed by an operator. The image point positioning is followed by a set of transformations, which convert 2D image co-ordinates into 3D global co-ordinates. An automatic alternative is designed for road signs inventory. This option employs step-wise processing: colour based object recognition and 3D positioning. The object recognition uses several image processing techniques: colour based segmentation, edge detection in colour space and automatic shape detection. Positioning is initiated by "Property Based Matching" and completed by image co-ordinate transformation into a global co-ordinate frame. The software was developed using object oriented Visual C++ language.

1. INTRODUCTION

Since 1970 the Swedish National Road Administration (SNRA) has been creating the Road Data Bank (RDB) for maintaining national roads (Bydler and Nilsson, 1979). In 1996, SNRA, National Land Survey, the National Defence Ministry and the Municipalities set up a project of building the National Road Data Base (NRDB). The NRDB will include information about all roads in Sweden. In a simplified form, one could present the NRDB as a digital map of Sweden with marked roads. Each road will include attributes such as owner of the road, road length and width, position of nodal points. With such a design, the NRDB will be a Geographic Information System (GIS) database (Isaksson, 1997).

In order to improve the efficiency of road data acquisition, SNRA searches for new data collecting systems. Up to now, SNRA has tested two types of Mobile Mapping Systems, land and airborne. For the purpose of road and road sign inventory only manual methods are used. Major source of information is data acquired by video is a. Recognition and registration of road and traffic signs are done by an operator (SNRA, 1995). Such monotone work benefits from automation. This paper describes automated road positioning, 3D point and vector measurement, and automatic extraction and positioning of road signs.

2. SYSTEM OVERVIEW

A Mobile Mapping System (MMS), is a modern solution for acquisition of data for Geographic Information System

(GIS). There are several mapping vans operating in reality. They differ in construction and quality of components, but the idea remains the same - GIS data acquisition; (Novak, 1995), (El-Sheimy et al., 1995), (Baraniak, 1995).

A typical MMS (Fig. 1) made up of three main sensors:

- GPS to determine 3D position of the platform in a global co-ordinate frame,
- INS to determine MMS platform attitude and to position the platform when received signal by GPS receiver is disturbed or lost (loss-of-lock),
- CCD camera system to capture the stereo image sequences of the road.

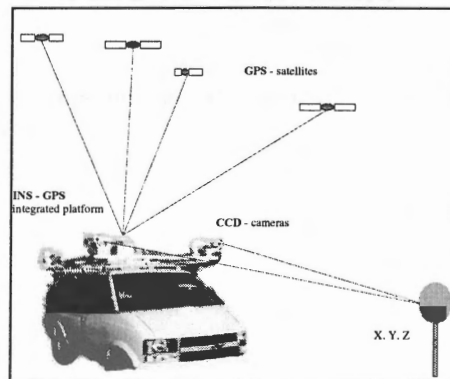


Figure 1. Mobile Mapping System.

Data post-processing is typically performed in two steps. In the first step, the GPS, INS, and odometer data are

processed. The results are global X, Y, Z co-ordinates of the GPS-phase centre, azimuth, pitch and roll - rotation parameters of the integrated sensors platform the MMS. These data are used in a second step - processing of stereo images. With the help of post-processing software developed within the project "Automation of road inventory using digital stereoscopic image analysis" (Gajdamowicz, 1997a), it is possible to measure the 3D co-ordinates of all object in the stereo image pair. A specially designed option enables automated inventory of road signs (Fig. 2).

The project described in this paper deals with data collected by the MMS "On-Sight" commercially available from Transmap Co., USA (Transmap, 1997). The colour image sequences were captured by colour progressive scan CCD cameras and time tagged with GPS/INS unit. Images were stored while driving at speeds of 72 km/h, 53 km/h and 30 km/h. The distance between captured stereo pairs was 15 m, 10 m and 5 m respectively.



Figure 2. The road sign - automatically recognised and positioned (in a global frame).

An accuracy of the system depends on the GPS/INS performance (Schwarz, 1995), the distance to the reference GPS receiver and the distance from the cameras to the inventory objects. Some practical tests have shown that inventory objects can be positioned with an accuracy of 0.3 - 2 m in a global frame (Gajdamowicz, 1997b). In the future images and 3D co-ordinates of inventory objects will be used as input to GIS data bases.

3. IMAGE ACQUISITION HARDWARE

Two Colour Progressive Scan cameras, Pulnix TMC-9700, (Fig. 3), are placed on the vehicle's roof. The camera's progressive scan property allows to acquire non-interlaced images of dynamic scene.



Figure 3. Colour Pulnix TMC-9700 camera.

The cameras are oriented in a way that allows to capture the stereo image pairs of a scene in front of the vehicle. The

baseline between the two cameras is two metres. Furthermore, the interior orientation parameters are established by self-calibration. The external orientation parameters are determined with integrated GPS/INS (He et al., 1992).

4. POST-PROCESSING OF GEOREFERENCED STEREO IMAGES

The inventory from georeferenced stereo images is performed in two basic alternatives: semiautomatic and automatic. The semiautomatic alternative is designed for task survey, a single 3D point measurement. This approach demands interaction between operator and software (Transmap, 1997).

An automatic alternative is designed for road signs inventory. This option employs step-wise processing, colour based object recognition and 3D positioning. The object recognition uses several image processing techniques like colour based segmentation, edge detection in colour space and automatic shape detection. Positioning is initiated by Property Based Matching (Section 4.3) and completed by image co-ordinate transformation into a global co-ordinate frame.

4.1 Automatic processing of image data; inventory of road signs.

4.1.1 Properties of a road sign

Road signs convey information to travellers through their shape, colour, message, and placement. The main properties of a road sign are colour, geometrical form and size (Fig. 4). The basic colours used for road signs are red, yellow, blue and green. These colours are backgrounds for traffic information:

- Yellow - used as background colour for warning signs.
- Blue - used as background colour for miscellaneous, traveller services and information signs.
- Green - used as background colour for guide signs.



Figure 4. Example of the Swedish road signs, typical geometrical shapes.

Visibility and readability of a sign depend on:

- background colour,
- colour of the text and symbols
- size of a sign
- size of text and symbols.

In addition, the shape of a sign is used for traffic guidance and information. The main geometrical forms used for signs are circular, triangular and rectangular. There are some particular forms like octagon, diamond, cross-buck and equilateral triangle, which are used for warning or yield purposes.

4.1.2 Segmentation based on colour

In automated image analysis, colour is a powerful descriptor that simplifies object identification and extraction from the

scene. The primary goal of colour segmentation in machine/computer vision is to determine where changes of material occur in a visual scene. In order to establish values which characterise the changes of material, relative colour differences have to be measured. There are several models for colour segmentation (Perez and Koch, 1994):

- physically based models,
- non-physically based models,
- hue space model.

Most of the models apply classical pattern-recognition techniques like histogram thresholding, clustering, region masking, etc.

Geiselman and Hahn (1994), presented a road sign segmentation method based on colour pixel classification into three classes: red, yellow and blue. Similarly, Yang (1995), uses RGB and HSI models for navigation of autonomous robots (model based on automatic recognition of colour landmarks).

In this project a step-wise process for segmentation of road signs is presented. The method employs:

- transformation from RGB to HSI domain,
- thresholding,
- morphological filtering,
- connected component analysis.

Basic threshold values for red, yellow, blue and green were measured from the test images.

The colours expressed in the RGB model are transformed to the HSI model (Bergholm, 1995). The HSI thresholds (Table 1) are applied to extract Regions Of Interest (ROI). The ROI can be defined as a group of black pixels corresponding to colour of road signs.

Sign	Colour	Value (byte range)	Limits
Green	Hue	41	15
	Saturation	255	30
	Intensity	from 25 to 225	
Blue	Hue	3	15
	Saturation	255	30
	Intensity	from 25 to 225	
Yellow	Hue	139	15
	Saturation	230	30
	Intensity	from 25 to 225	
Red	Hue	180	15
	Saturation	255	30
	Intensity	from 25 to 225	

Table 1. Threshold values for colours used in segmentation of the road signs.

The ROIs are the best candidates for further processing. Unfortunately, images acquired in outdoor environment contain noise. Noise, in this approach, is all colour information that is let through the threshold, but does not correspond to the road sign. There are some main sources of noise:

- road paintings,
- paintings on buildings,
- information boards and advertisement signs,
- cars.

One way to reduce noise is to use morphological filtering. The morphological opening and closing filters were used. In case where segmented sign consists of more than one colour and is rich in symbols and text, analysis become more complex. Straightforward morphological filtering can break ROIs into several elements. To avoid splitting of ROIs into

sub-regions, connected component analysis followed by additional thresholding should be carried out.

All connected objects in the image are created in an iterative process, using 8-connectivity between pixels (Gonzales et al. 1993). When the criteria of connectivity are fulfilled, minimum rectangles enclosing connected objects are computed. This completes the segmentation (Fig. 5).

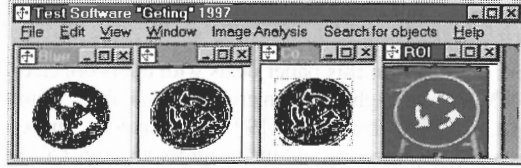


Figure 5. Step-wise segmentation: thresholding, connected component analysis, additional thresholding, minimum enclosing rectangle, segmented ROI.

4.2 Automatic detection of circular, rectangular and triangular forms

Automatic detection of the boundaries of signs is mainly based on edge extraction in colour space, histogram analysis and edge linking through Hough transformations. As mentioned in Section 4.1.2, connected component analysis enables ROI to be enclosed with the minimum rectangle. In the next step, the region within the rectangle is referred to the original image. From now on an algorithm will work locally within ROI.

4.2.1 Detection of edges in HSI space

Edge detection in the HSI domain has been investigated lately by Perez and Koch (1994), Scharcanski (1995) and Yang (1995). The edge in a colour image is a boundary between two regions with relatively distinct hue (saturation). Basically, the idea underlying edge detection in HSI domain is the computation of local derivatives. This is performed in three separate grey-level images, i.e. hue image, saturation image and intensity image.

4.2.1.1 Mathematical model

Let us represent a colour image, transformed into HSI domain as an intensity function

$$I_{(HSI)}(x, y) = G_H, G_S, G_I \quad (1)$$

where G_H is a hue grey-intensity image, G_S refers to saturation and G_I to intensity grey-scale image. The gradient of function $I_{(HSI)}(x, y)$ is, by definition, the vector $\vec{\nabla} I_{(HSI)}(x, y)$ and can be presented as:

$$\vec{\nabla} I_{(HSI)}(x, y) = \begin{bmatrix} \frac{\partial G_H}{\partial x} & \frac{\partial G_H}{\partial y} & \frac{\partial G_S}{\partial x} & \frac{\partial G_S}{\partial y} & \frac{\partial G_I}{\partial x} & \frac{\partial G_I}{\partial y} \end{bmatrix} \quad (2)$$

Assuming that the sampled intensity surface is continuously differentiable, then the simplest way to devise difference operators is to estimate directional derivatives:

$$\Delta_1 = \left(\frac{\partial G_H}{\partial x} \right), \Delta_2 = \left(\frac{\partial G_H}{\partial y} \right), \Delta_3 = \left(\frac{\partial G_S}{\partial x} \right), \Delta_4 = \left(\frac{\partial G_S}{\partial y} \right), \Delta_5 = \left(\frac{\partial G_I}{\partial x} \right), \Delta_6 = \left(\frac{\partial G_I}{\partial y} \right) \quad (3)$$

of image intensity. Then, the magnitude of gradient is:

$$\Delta_{(HSI)} = \sqrt{\left(\frac{\partial G_H}{\partial x}\right)^2 + \left(\frac{\partial G_I}{\partial x}\right)^2 + \left(\frac{\partial G_S}{\partial x}\right)^2 + \left(\frac{\partial G_H}{\partial y}\right)^2 + \left(\frac{\partial G_I}{\partial y}\right)^2 + \left(\frac{\partial G_S}{\partial y}\right)^2} \quad (4)$$

and the direction of image-intensity gradient with respect to ∇I_1 :

$$\alpha_{(HSI)} = \arctan \left[\frac{\left(\frac{\partial G_H}{\partial y}\right)^2 + \left(\frac{\partial G_I}{\partial y}\right)^2 + \left(\frac{\partial G_S}{\partial y}\right)^2}{\left(\frac{\partial G_H}{\partial x}\right)^2 + \left(\frac{\partial G_I}{\partial x}\right)^2 + \left(\frac{\partial G_S}{\partial x}\right)^2} \right] \quad (5)$$

4.2.1.2 Implementation of the Mathematical Model

The colour edge detection is initiated, as mentioned in Section 4.2.1.1, by transformation into HSI domain. Then, before using the normal gradient method, the grey-scale images (G_H, G_I, G_S) are smooth. Each of the G_H, G_I, G_S images is smoothed using a simple (3x3) averaging filter. Averaging decreases the presence of minor edges. When smoothing has been applied to the hue, saturation and intensity images the gradients are calculated, using directional difference operators, i.e. $\Delta_{I_{1...6}}$ (Fig. 6). In this approach, the Sobel operators in horizontal and vertical directions are used.

Due to the circular nature of hue, a supplementary procedure needs to be implemented. The gradient operators in hue normally create false edges for hue angles around 0 and 2π . Hence, this passage does not correspond to the border between colours. The following formula can be used to eliminate false edges:

$$G_H \cdot A \cdot \Delta_1 = H_{false} \Rightarrow H_{real}(x, y) = 2(\pi - abs(H_{false}(x, y) - \pi)) \quad (6)$$

where x, y correspond to image co-ordinates.

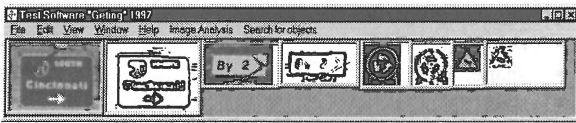


Figure 6. Thresholded edges detected from colour images.

HSI space has advantages compared to RGB mainly due to properties of hue (Perez et al. 1994):

- multiplicative/scale invariance:

$$\forall \theta > 0 \wedge (\theta S, \theta M, \theta L) \in [0, 2\pi] \Rightarrow hue(S, M, L) = hue(\theta S, \theta M, \theta L) \quad (7)$$

- additive/shift invariance:

$$\forall \beta \rightarrow (S + \beta, M + \beta, L + \beta) \in [0, 2\pi] \Rightarrow hue(S, M, L) = hue(S + \beta, M + \beta, L + \beta) \quad (8)$$

Thus, edges will be invariant to shadows, highlights and transparency. Therefore, the HSI model is suitable for treating outdoor colour images.

4.2.2 Automatic curve detection

In this section a practical approach to fitting curves to edgel data will be presented. The Hough transform was proposed

as early as 1962 (Duda and Hart, 1972) and is since then successfully used for curve fitting. The underlying idea is as follows: suppose that we are given a set of points (edges), such as points with assigned tangents - and we know the parametric form of the curve to which these points belong. Then, the parameters of the curve can be determined in two steps. In the first step, each point is mapped on to the set of all parameter values, for which the curve passes through the given point. In the second step, the intersection of all the sets of parameter values are mapped. This intersections approximate the values of the underlying curve.

4.2.2.1 Circles

The Hough transform for circles is used to detect circular shapes. The circle can be described by three parameters, coordinates of centre point $C_p (x_{C_p}, y_{C_p})$ and radius R . Our task is to estimate the parameters for all possible circles passing through the points (edges) in the smoothed gradient image.

Let us describe a circle with the following equation:

$$(x_p - x_{C_p})^2 + (y_p - y_{C_p})^2 = R^2 \quad (9)$$

The accumulator matrix is the 3D parameter space with elements R, x_{C_p}, y_{C_p} , which divides the accumulator into cells (Fig. 9). Then, let us define the size of an accumulator as $(x_{bins}, y_{bins}, r_{bins})$.

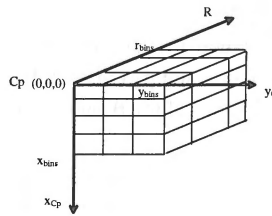


Figure 7. The 3D accumulator.

Initially, the cells are set to zero, but every time the curve parameter is computed, the indexed cell is increased by one.

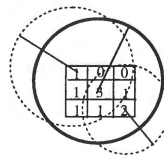


Figure 8. Indexed accumulator with the best circle.

When indexing is completed, the accumulator cell with the highest value is selected (Fig. 8). The index of the best cell is further used to compute the best circle (Eq. 9). Lastly, the circle is painted on the original image (Fig. 9).

The circle detection is moreover improved by testing if the circle's radius is perpendicular to the gradient direction of the estimated circles edge and by limiting the size of accumulator.



Figure 9. Automatically detected circles.

4.2.2.2 Rectangles

Automatic detection of rectangular shapes fits the best rectangle to the horizontal and vertical edges of gradient image (Fig. 10). Initially, the gradient image needs to be divided into two images, one containing horizontal edges and the other containing vertical edges. Then, two horizontal lines making up the upper and lower bound of the rectangle are found by histogram analysis. A similar procedure is repeated for vertical edges (Öhman, 1998).

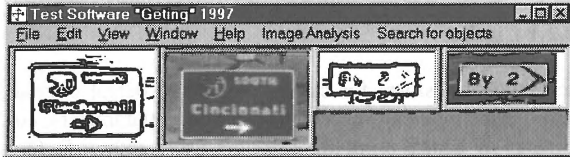


Figure 10. Automatically detected rectangles.

4.2.2.3 Triangles

As in automatic detection of circles, the Hough transform is applied for detection of triangles. Similarly to previous methods, the gradient image is computed from colour ROI. Further, three line equations are derived in order to find the contours of a triangle.

The line is represented by the normal equation:

$$x \cos \theta + y \sin \theta = \rho \quad (10)$$

where ρ is the perpendicular distance to the line and θ corresponds to the angle between x axis and ρ (Fig. 11). For the points in the gradient image, the values θ and ρ are computed.

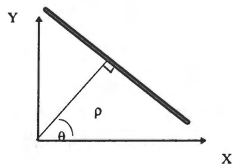


Figure 11. Normal representation of a line.

These numbers are mapped into 2D accumulator space. The size of the accumulator defines the range of angles $\theta \in (-\pi, \pi)$ and $\rho \in (-\sqrt{2}d, \sqrt{2}d)$.

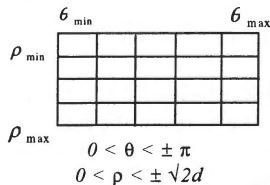


Figure 12. Quantization of the $\rho\theta$ plane into cells.

The value d , in case of this application, is the width of the ROI. The highest value in the accumulator indicates (Fig.12) the best line. The triangular road signs have the form of a regular triangle where the angles between sides are equal to $\frac{2}{3}\pi$. Therefore, one can put a slope condition to detect lines

with the slope π , $\frac{2}{3}\pi$ and $\frac{4}{3}\pi$ only. For the triangles, which are inverted a minus sign is introduced to the slope angles.

Three lines detected in such a procedure cross each other at three points, which correspond to the corners of a triangle. Moreover, from these points the centre of road sign is calculated. In the final step the triangle is painted in the original image (Fig 13).

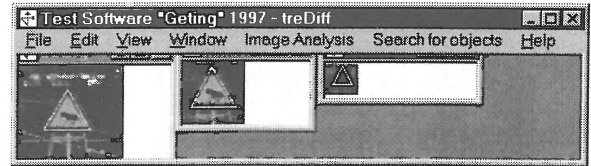


Figure 13. Automatically, extracted triangular road signs.

4.2.3 Quality measure for the detected shapes

In order to automatically evaluate detected forms, the quality factor has to be derived. The quality (q) corresponds to number of black pixels (edges) on the detected boundary (Eq. 11).

$$q = \begin{cases} 0 & \text{if } p < 50 \\ \frac{p}{100} & \text{otherwise} \end{cases} \quad (11)$$

If a boundary consists of gradient edges only ($p=100\%$), then the (q) will equal 1. If a boundary include 80% edges, then quality is 0.8. For values less than 0.5, shape determination rejects all possible shapes.

4.3 Automatic positioning of road signs

The 3D position of a sign is determined with newly developed "Property Based Matching" (PBM). The PBM is a knowledge based algorithm, which finds corresponding objects (road signs) in a stereo image pair and then determines their 3D position.

The PBM finds the correspondence between road signs by comparing sign properties (Section 4.1.1):

- colour,
- shape,
- size.

The best match corresponds to signs (ROIs) with the same colour, shape and size.

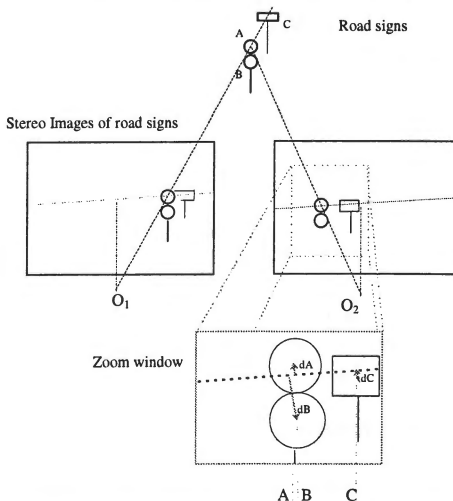


Figure 14. Principles of sign positioning.

Unfortunately, there are cases when the PBM finds several best matches, for example, two round circular signs above each other (Fig. 14). In such a case, the following processing is applied:

- computation of epipolar line,
- computation of the perpendicular vector from the centre of sign to epipolar line,
- monotonic-ordering (Nalwa, 1993).

In order to match sign "A" from the left image to the right one, PBM employs following:

1. For the sign "A" in the left image the centre point is calculated.
2. For the calculated centre point the epipolar line is computed in the right image as follow:

Let us assume x_l, y_l, z_l to be the left camera image co-ordinates (origo in projective centre) and x_L, y_L to be CCD pixel co-ordinates (origo in left lower corner of the image). Next, let matrix A_L represents transformation (internal calibration) from pixel co-ordinates to the image plane co-ordinate system (Eq. 12).

$$\begin{bmatrix} x_l \\ y_l \\ z_l \end{bmatrix} = A_L \begin{bmatrix} x_L \\ y_L \\ 1 \end{bmatrix} = -f_{x,L} \begin{bmatrix} -1 & 0 & X_{c,L} \\ f_{x,L} & 0 & f_{x,L} \\ 0 & -1 & Y_{c,L} \\ 0 & 0 & f_{y,L} \\ 0 & 0 & 1 \end{bmatrix} \begin{bmatrix} x_L \\ y_L \\ 1 \end{bmatrix} \quad (12)$$

where calibration coefficients are :

- * $(X_{c,L}, Y_{c,L})$ - centre of an image (CCD array) i.e., pixel index for intersection between CCD plane and an optical axis (z_l -axis).
- * $f_{x,L}, (f_{y,L})$ - focal length of the camera expressed in pixels in $x_L, (y_L)$ direction.

Then, the essential matrix E is derived from the relative position of cameras by $E = T_l R$ where T_l is the skew-symmetrical matrix:

$$T_l = \begin{bmatrix} 0 & T_{31} & -T_{21} \\ -T_{31} & 0 & T_{11} \\ T_{21} & -T_{11} & 0 \end{bmatrix} \quad (13)$$

The relation between corresponding points in the left and right image is derived applying the coplanarity condition:

$$\begin{bmatrix} x_l & y_l & z_l \end{bmatrix} E \begin{bmatrix} x_r \\ y_r \\ z_r \end{bmatrix} = 0 \quad (14)$$

The Eq. 14 in terms of pixel co-ordinates can be written as:

$$\begin{bmatrix} x_L & y_L & 1 \end{bmatrix} A_L^T E A_R \begin{bmatrix} x_R \\ y_R \\ 1 \end{bmatrix} = 0 \quad (15)$$

Finally, for given x_L, y_L pixel co-ordinates in left image one can compute the epipolar line which passes through the corresponding point in the right image (Eq. 15).

3. For every sign the perpendicular distance from its centre point to the epipolar line is calculated .

The road sign, whose centre is within the shortest distance to the epipolar line, is the best match. Finally, monotonic-

ordering is invoked. The monotonic-ordering assumes that conjugate points along corresponding epipolar lines has the same order in each image (Fig. 14). In order to avoid violation of monotonic-ordering assumption, condition, stating that the area of corresponding signs must be the same, was implemented.

4.3.1 Transformation to a global frame

Automatic processing of sign extraction is completed by positioning in a global frame (Fig. 15).

1. The first transformation is the transformation from pixel co-ordinates to image co-ordinates system, (Eq. 12). This transformation is performed for both cameras.
2. In the second step, the model co-ordinates are solved using interior and exterior orientation parameters (Fornland, 1996).
3. In the next step, the model co-ordinate system is transformed to mobile platform co-ordinate system:

$$P_v = T_v + R_v (R_{system} P) \lambda \quad (16)$$

where:

- P - model co-ordinates,
- P_v - mobile platform co-ordinates ,
- T_v - translation,
- R_v - rotations,
- λ - scale factor.

4. Finally, the mobile platform co-ordinate system is transformed to the global co-ordinate system.

$$P_G = T + R_{A,P,R} P_v \Lambda \quad (17)$$

where:

- P_G - global co-ordinates,
- T - translation,
- $R_{A,P,R}$ - rotations (azimuth, pitch, roll),
- P_v - mobile platform co-ordinates,
- Λ - scale factor.

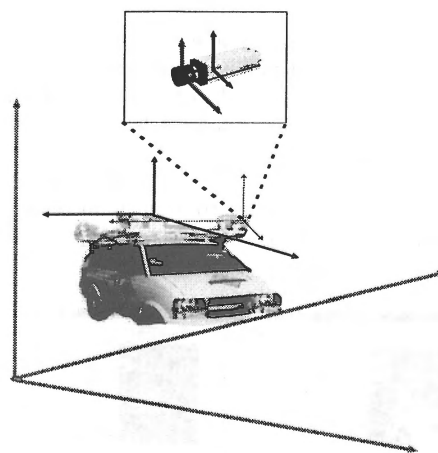


Figure 15. Transformations of 2D image co-ordinates to 3D global frame.

The 3D global co-ordinates are displayed in a result window together with the images of the corresponding road signs. Additionally, the result window includes information about image co-ordinates, form, size (area) and colour of the road sign.

4.4 Manual inventory of roads

Road scenes are complex. Some objects, like road signs, are clearly visible. Thus, automatic identification is in most cases possible. Unfortunately, there is a group of other objects like:

- barriers
- kerbs,
- pavements,
- buildings,

which are very difficult to detect and classify (from image data only). Complicated structures, lack of significant colours, low/high saturation makes automatic detection and positioning of objects in a 3D global co-ordinate frame problematic (Section 4.3).

For such a scenario, a manual option was designed. Similar approaches have been implemented in MMS softwares like STEPS (Transmap, 1996), GEOstation (Geofit, 1996), GPSVision (Lambda Tech, 1996).



Figure 16. The stereo image pair. P0 (in upper image) is a selected feature.

In order to express the position of an object in 3D global co-ordinates, human interaction is sometimes required. Initially, an observer has to recognise the object in one of the images (Fig. 16). Then, an object needs to be marked, image co-ordinates are computed.

To support the manual image co-ordinate measurement, the zoom window interface has been designed and implemented (Fig 17).

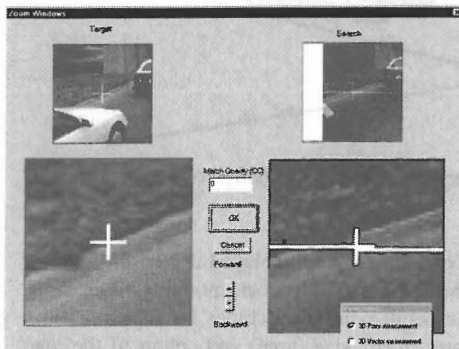


Figure 17. Zoom window.

After selecting a point in the left image, the corresponding epipolar line is computed in the other image. The corresponding point along the epipolar line (in the right image) is found by manual targeting or by template matching. Unfortunately, matching can give multiple answer, e.g., if the target or the template has too low saturation.

In addition to single 3D point measurement, 3D vector measurement option can be selected. This option is mainly design for 3D distance measurement between inventory objects, e.g. road width measurement. The 3D vector measurement needs to be initiated by manual selection of two 3D points, between which the distance is calculated.

5. CONCLUSION

This paper has presented automated methods for processing of colour stereo georeferenced images collected by the Mobile Mapping System "On-Sight".

The methods for automated 3D point (vector) measurement and automatic road sign inventory were developed and implemented into object oriented software. The methods enable inventory of roads; positioning of the inventory objects in a global co-ordinate frame.

The method for 3D point (vector) measurement requires human interaction by selecting an object in the image. For clearly visible objects template matching can be applied in order to support human operations.

The automatic method is specially designed for detection and positioning of Swedish road signs. Signs are extracted based on step-wise processing such as colour based segmentation, automatic shape detection and Property Based Matching.

The accuracy of inventory objects in a global co-ordinates is influenced by the accuracy of GPS/INS data, interior calibration parameters and by the distance from the inventory object to the camera system. The accuracy of the image point extraction (automatic or manual) has a minor effect on the global precision of the measurement. Therefore, evaluation of precision for the image point extraction was not included in this paper. The global accuracy of the system is within 0.3 - 1 m range (for objects up to 20 m from the cameras).

ACKNOWLEDGEMENTS

The author is grateful to the Swedish National Road Administration; Lars Lindqvist and Per Isaksson, for financing this project; and to professor Kennert Torlegård for his supervising. Special thanks Dr. Kurt Novak (Transmap Co.) for help with data acquisition and to Daniel Öhman (KTd Visual Solutions) for his skilful programming contribution while implementing algorithms due to segmentation, Hough transform and positioning.

REFERENCES

Baraniak D.W., 1995. GPSVision A state of the art MMS system. Proceedings 1995 Mobile Mapping Symposium, The Ohio State University & Department of Geodetic Science and Survey, USA, pp-256

- Bergholm F., 1995. Tools for Colour. Illumination and Motion Analysis in Compute Vision - an Introduction. CVAP-TN 18, Technical Note from Computational Vision and Active Perception Laboratory (CVAP), Sweden, pp 1-37.
- Blaho G. Charles C., 1995. Field Experiences with Full Digital Mobile Stereo Acquisition System. Proceedings 1995 Mobile Mapping Symposium, The Ohio State University & Department of Geodetic Science and Survey, USA, pp 97-105.
- Bydler R., Nilsson A., 1979. The Swedish Road Data Bank its use in road planning. Internal Report. National Swedish Road Administration. Borlänge, Sweden.
- Duda R., Hart P. 1972., Use of Hough Transformation to Detect Lines and Curves in a Pictures. Communications of the ACM, Vol. 15, No. 1(January), pp 11-15.
- Fornland P., 1996. Frilab - DSFK. Laboratory notes. Computational Vision and Active Perception Laboratory (CVAP), NADA-KTH, Sweden.
- Gajdamowicz K., 1997a. Automation of Road Inventory Using Stereoscopic Image Analysis. Proceedings Symposium on Image Analysis, SSAB 1997. KTH. Stockholm, Sweden, pp 139-144.
- Gajdamowicz K., 1997b. Reference Group Meeting No 3. Internal Report. Dept. of Geodesy and Photogrammetry. KTH. Stockholm, Sweden,.
- Geiselman Ch., Hahn M., 1994. Identification of Simple Object in Image Sequences. International Archives of Photogrammetry and Remotesensing, Commission III, Germany. pp 288-295.
- Geofit., 1996. Proposal submitted to Royal Institute of Technology. Canada.
- Gonzalez R.C, Woods. R.E., 1993. Digital Image Processing. Addison-Wesely Publishing Company, USA p 716.
- He G., Novak K., and Feng W., 1992. On the integrated calibration of a digital stereo-vision system. International Archives of Photogrammetry and Remotesensing, Commission V, pp 139-145.
- He G., Novak K. and Feng W.,1992. The accuacy of features positioned with the GPSVan. International Archives of Photogrammetry and Remotesensing, Commission II, pp 480-486.
- Isaksson M. Olund P., 1997. Nationell Vägdatabas (NVDB). Homepage of the National Swedish Road Administration. <http://www.vv.se/vdatabas/vdatabas.htm>.
- Lambda Tech., 1996. Product information, background, service guide. Information Brochure, USA.
- Nalwa V.S., 1993. A guided tour to computer vision. Addison-Wesly Publishing Company. ISBN 1-201-54853-4., p 361.
- Novak K., 1995. Mobile Mapping Technology for GIS Data Collection. American Society for Photogrammetry and Remotesensing, Vol. 61, No. 5, pp. 439-501.
- Perez F., Koch Ch., 1994. Toward Segmentation in Analog VLSI: Algorithm and Hardware. International Journal of Computer Vision, Kulver Academic Publisher, Vol 12. Boston USA, pp 17-42.
- Piccioli G., De Micheli E., and Campani M., 1994. A robust method for road sign detection and recognition. Lecture Notes in Computer Science, Vol. 800. Computer Vision - ECCV 94,pp 495-500.
- Pulnix. 1997.
Homepage at <http://www.pulnix.com/tmc9700.htm>.
- Scharcanski J. and Venetsanopoulos A.N., 1995, Colour Image Edge Detection Using Directional Operators. Proceedings of 1995 IEEE Workshop on Nonlinear Signal and Image Processing.
- Schwarz K.P, El-Sheimy N., 1995. INS/GPS present state. Proceedings 1995 Mobile Mapping Symposium, The Ohio State University & Department of Geodetic Science and Survey, USA.
- SNRA, the Swedish National Road Administration., 1995. Internal Report. PC-VDB Fäldator. Vägdatbanken. Sweden.
- Transmap., 1997. ON-SIGHT Mobile Mapping System. Homepage. <http://www.transmap.com/technoloy.htm>
- Öhman D., 1998. Automatic Text Localisation from Colour Stereo Image Sequences. MSc Thesis. Dept. of Geodesy and Photogrammetry. KTH, Stockholm, Sweden.
- Yang H., 1995. Vision Methods for Outdoor Robot Navigation. PhD Thesis. . ISSN 0783-5477. Helsinki University of Technology. Finland.